Desalination and Water Treatment
www.deswater.com

doi: 10.5004/dwt.2022.28145

249 (2022) 281–296
February

Amberlite IRA-93 and modified Amberlite IRA-93 resins for the uranyl ions extraction: optimization through factorial design methodology

Yasmine Benmansour, Mohamed Amine Didi*, Omar Abderarhim

Laboratory of Separation and Purification Technologies, Department of Chemistry, Faculty of Sciences, Box 119, University of Tlemcen, 13000 Algeria, Tel. +213 552639237; email: madidi13@yahoo.fr/ma_didi@mail.univ-tlemcen.dz (M.A. Didi)

Received 2 September 2021; Accepted 5 January 2022

ABSTRACT

This work reports the uranyl (UO_2^{2+}) extraction from water by the resins Amberlite IRA-93 (A-IRA-93) and the new modified Amberlite IRA-93 (mA-IRA-93), by liquid-solid extraction. A comparative study investigated the extraction procedure for the solid phase extraction of toxic uranyl ions by both the Amberlite IRA-93 (A-IRA-93) and the modified Amberlite IRA-93 (mA-IRA-93) resins in a batch process. The effect of solution pH, contact time, initial uranyl concentration, ionic strength and temperature were evaluated. The extraction process followed a pseudo-second-order kinetics models for both resins. The thermodynamics data led to an endothermic process for the sorption of uranyl ions by both resins. Thermodynamic study showed a negative ΔG values for A-IRA-93 and mA-IRA-93, which indicated that the sorption process of uranyl ions was spontaneous. The ratio $\Delta G_{\text{mA-IRA-93}}/\Delta G_{\text{A-IRA-93}}$ = 10.58 shows that the extraction by the mA-IRA-93 was more spontaneous than the extraction by the A-IRA-93. The outcomes have shown that the optimal experimental conditions without addition of sodium acetate for the present study recommend the use of 0.03 g of A-IRA-93 and 0.02 g of mA-IRA-93 resins for initial uranyl concentration 10^{-4} mol L^{-1}. Fractional experimental design $3^{(3-1)}$ may provide a valuable basis for industrial scale applications and was adequate in this study. The best extraction yield for mA-IRA-93 resin was 100% at 3.5 pH_i and an equilibration time of 30 min at 250 rpm, provided by experiment: w(mA-IRA-93) = 0.01 g, $[UO_2^{2+}] = 10^{-5}$ mol L^{-1} and $[CH_3COONa]$ = 0.2 mol L^{-1}. Modified Amberlite IRA-93 showed better affinity towards UO_2^{2+} (a maximal capacity of 8.34 mg g^{-1}) under optimum conditions. Modification of the resin Amberlite IRA-93 increases the retention capacity by a factor of 2.21. The two proposed adsorbents are cost-effective and environmentally friendly and potential candidates for treatment of water containing UO_2^{2+}. The functionalized adsorbent (mA-IRA-93) has research value and application potential in real waste water treatment.

Keywords: UO_2^{2+}; Extraction; Amberlite IRA-93 resin; Optimization

1. Introduction

Water contamination with toxic ions is becoming a great environmental concern. Therefore, clean and non-contaminated water with permissible levels of metal ions has drawn to develop effective technologies for toxic ions removal from water solutions. Uranium is a heavy metal that can be found at low levels within many rocks, sediments and soils. The average U concentration in the earth crust is between 2 and 4 ppm, but it can be enriched in soil and groundwater by several anthropogenic activities, such as by the release from mill tailings of U mines, or by agricultural application of phosphate fertilizers, which are often, associated with U or by nuclear industries wastes [1]. It is also one of the most commonly detected radioactive elements in water and wastewater, so it has attracted wide concern [2]. Hence, several studies have been made to evaluate U toxicity and

* Corresponding author.

bioaccumulation in animal and plant samples exposed to water-only U concentrations [3–7]. It is in fact a hazardous contaminant in the environment due to its radioactivity and toxicity (carcinogenic for humans). Thereby, the World Health Organization (WHO) recommends a drinking water limit of 0.015 mg L^{-1} [8].

The existence of highly mobile hexavalent uranium (U(VI)) in the aquatic environment would exceedingly hazard human being and natural ecosystems [9,10]. In order to avoid serious harm to mankind, it is highly desirable to find a promising efficient approach for U(VI) removal from water.

Many water purification technologies including photocatalysis, ion exchange, and the solid phase extraction (SPE), etc. [11–14] have so far been implemented to treat U(VI) contamination. SPE is regarded as one of the simple and most effective pre-concentration procedure among these technologies, due to its simplicity operating and environmental friendliness [15–20]. Solid phase extraction of uranium is also a preferable choice in the analytical chemistry [21–23].

Several properties of SPE such as selectivity, simplicity of equipment, ease of operation and the multiple usages of adsorbents for numerous separations and preconcentration cycles without deprivation in the metal ion sorption capacity have made their use popular [24–29].

Many resins have been used for the removal of uranyl such as XAD-2010 [30], and ethylenediamino tris(methylene phosphonic) acid grafted on polystyrene [21].

The Amberlite IRA-93 resin was used for solid phase extraction studies of heavy metal ions [30] in the environmental samples. But it has never been used in the extraction of uranyl, especially with this new functionalized form. It is a macroporous (particle size, 0.25–0.7 mm) styrene-divinylbenzene co polymeric backbone with tertiary amino groups, and also a weak anion exchange resin defined as an adsorbent resin of the acrylic type [11].

The objective of our work is the extraction and isolation of uranyl ions by a new effective and practical suitable sorbent. We will mainly focus on the comparison of the two resins Amberlite IRA-93 (A-IRA-93) and its modified form (mA-IRA-93) by grafting it with dimethylenephosphonic acid (DMPA), we will also describe its synthesis (Fig. 1) and its characterization.

The effects of analytical parameters, adsorption kinetic, isotherm studies and temperature effect will be investigated. Fractional experimental design $3^{(3-1)}$ was used in this study in order to define the operating conditions corresponding to the best extraction yield of uranyl ions.

2. Materials and methods

2.1. Reagents

All solutions were prepared from analytical grade chemicals and distilled water. Commercially Amberlite IRA-93 resin (CAS No. 9036-92-4, purity 99%), was purchased from Polysciences, Inc. Uranyl acetate dehydrate ($UO_2(CH_3COO)_2 \cdot 2H_2O$, (Mw = 426.13 g mol^{-1}, purity ≥ 98%), arsenazo III ($C_{22}H_{16}As_2N_4O_{14}S_2$, Mw = 774.34 g mol^{-1}, purity ≥ 99%) acetic acid (Mw = 60.052 g mol^{-1}, purity = 99.5%), hydrochloride acid (37%) and ammonium acetate (purity ≥ 97%) were provided from Sigma-Aldrich. Phosphorous acid (purity = 98%) and formaldehyde were purchased from Riedel-de Haën and Gifrer-Barbezat respectively. Sodium hydroxide (≥97.0%, pellets), sodium chloride and sodium acetate were purchased from Prolabo Rectapur.

A stock solution of 10^{-3} mol L^{-1} of $UO_2(CH_3COO)_2 \cdot 2H_2O$ was prepared by dissolving 0.4241 g in 1 L of distilled water. The diluted solutions of uranyl ions were prepared by appropriate dilution of the stock solutions. The initials pH of the sample solutions were adjusted in the desired range by adding dilutes of CH_3COOH or NaOH solutions.

2.2. Apparatus

All pH measurements were performed with a WTW 3310 Set 2 digital pH meter. The extraction of UO_2^{2+} on resins was studied by batch technique. A shaker (Haier model) was used for removal experiments except for temperature effect where a magnetic stirrer (RCT basic IKAMAG stirrer with ETS-D5 temperature controller) was used. Specord® 210 Plus model analytic Jena UV-Vis spectrophotometer was used to determine UO_2^{2+} as M^{n+}–Arsenazo III complex in aqueous phase [32–34] and PFP7 Flame Photometer JENWAY was used to determine Na^+ concentration. Fourier transform infrared (FT-IR) spectrum was recorded on a Agilent technologies Cary 360 spectrometer. Field-emitting scanning electron microscopy (SEM) images were carried out by a HITACHI TM-1000 Tabletop microscope. A phase analysis of a powder sample was carried out by a X-ray powder diffraction measurements on a Model Rigaku-Miniflex 600 using Ni filtered Cu Kα radiation (λ = 1.5406 Å). The study was done between 2° to 79° 2θ values with step size 0.02 and a scan speed of 4°/min^{-1}. A Bruker Advance 400 spectrometer was used for ^{31}P MAS NMR analysis. Gas sorption measurements were obtained from an 3Flex Version 5.00 adsorption analyzer (Micromeritcs) by using N_2 at 76,964 K (liquid N_2 temperature). The samples were degassed at 423 K for 8 h.

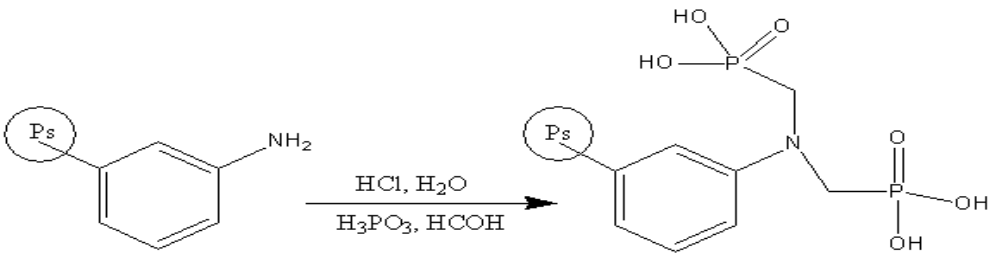

Fig. 1. Scheme for synthesis of mA-IRA-93 resin.

The Brunauer–Emmett–Teller (BET) method was applied for total surface area evaluation and the pore size.

The statistical study of this plan was carried out by Statistica 12.

2.3. Synthesis of Amberlite IRA 93 anchored with di(methylene phosphonic) acid

The new sorbent, mA-IRA-93 was synthesized using the Moedrizer-Irani reaction [21] (Fig. 1).

In a reactor fitted with a condenser, a mixture of hydrochloric acid 37% (18 mL), phosphorous acid (13 g) and 15 mL of distilled water, was vigorously stirred in order to dissolve completely the phosphorus acid. The solution was added to a 10 g of A-IRA-93 resin and an aqueous solution of formaldehyde (15 mL, 37%) was added and refluxed for 5 h. The resulting polymer was filtered and washed with distilled water and dried under vacuum [35].

2.4. Extraction and analysis procedure

In aqueous phase, the UO_2^{2+} concentrations were determined spectrophotometrically with Arsenazo III. In a test tube, which contained 2 mL of ammonium acetate/HCl buffer at pH = 2.0 [21], were added to 100 μL of UO_2^{2+} solution to be analyzed and 100 μL of Arsenazo III solution at 10^{-3} mol L^{-1}. Arsenazo III reacts with UO_2^{2+} to form a blue complexe which can be estimated at λ_{max} = 651 nm [17,20].

The general method of extraction, used for this study, was described as follows: 0.03 and 0.02 g of A-IRA-93 and mA-IRA-93 resins respectively were equilibrated with 4 mL of uranyl ions solution of known concentration in a stoppered Pyrex glass flask at a temperature of (22°C ± 1°C) in a shaker for duration of 60 min. The choice of resin masses was made after carrying out several tests beforehand, and the best yields of extraction were found with these masses for each of the resin.

The resin was separated by filtration and the filtrate was analyzed by UV-Vis spectrophotometer in presence of Arsenazo III for uranyl ions content [17].

The extraction of UO_2^{2+} ions on the resin at four different temperatures 20°C, 30°C, 40°C and 50°C was investigated. For temperature effect, a magnetic stirrer was used and stirring speed was 250 rpm to maintain resin particles in suspension. All data reported are based on the average of three replicate measurements.

The percentage of metal ions that was sorbed on the resin (i.e., extraction yield, Y (%)) was determined by comparing its concentrations before and after extraction [Eq. (1)] [17].

$$Y(\%) = \frac{C_i - C_e}{C_i} \cdot 100 \quad (1)$$

where C_i is the initial uranium concentration and C_e its equilibrium concentration.

The amount of metal uptakes at time t, q_t (mg g^{-1}), was calculated by Eq. (2) [17]:

$$q_t(\text{mg g}^{-1}) = \frac{C_i - C_t}{w} \cdot V \quad (2)$$

where C_i and C_t are respectively the initial and time t, V is the volume of the solution, w is the mass of the resin used.

The distribution coefficient (K_D) of the uranyl ions between the aqueous solution and the solid resin was also calculated from Eq. (3) [17]:

$$K_D\ (\text{mL g}^{-1}) = \frac{[M]_{\text{resin}}}{[M]_{\text{aq}}} = \frac{C_i - C_e}{w} \cdot V / C_e \quad (3)$$

where $[M]_{\text{resin}}$ and $[M]_{\text{aq}}$ were UO_2^{2+} ions concentrations in resin phase (mg g^{-1}) and in aqueous solution (mol L^{-1}), respectively. C_i, C_t and C_e are respectively the initial, time t and equilibrium, UO_2^{2+} concentration (g L^{-1}). V is the volume of the solution (4 mL). w is the mass of the resins used 0.02 g of A-IRA-93 and 0.03 g of mA-IRA-93.

3. Results and discussion

3.1. Characterization studies

In the FT-IR spectra, the presence of phosphonic acid was confirmed by the appearance of elongation absorptions at ν_s (O–H) = 3,425 cm^{-1}, ν_s (P=O) = 1,017 cm^{-1}, and ν_s (P–OH) = 942 cm^{-1} [35,36] with the disappearance of NH_2 band at ν_s = 2,925 cm^{-1}.

The ^{31}P MAS NMR spectrum of mA-IRA, recorded at as pinning rate of 14 KHz showed one peak of high intensity at 0.9 ppm, attributed to the phosphonic $PO(OH)_2$ units.

The morphologies and size distributions of the A-IRA-93 and mA-IRA-93 resins were characterized by SEM (Fig. 2) and X-ray diffraction (XRD) (Fig. 3), respectively. The resins are spherical (Fig. 2a and c) with a symmetric and medium size (250–500 μm), and have micropores on their surface (Fig. 2b and d).

XRD diagrams and isotherms of the A-IRA-93 and the mA-IRA-93 resins are presented in Figs. 3 and 4. Textural and structural parameters of both resins used in this study are given in Table 1.

The resins present a hexagonal structure with low surface area and high pore size. After the functionalization, a slight decrease in the unit cell parameter of the solid is observed but the hexagonal structure is maintained. The N_2 isotherm of A-IRA-93 was not different from mA-IRA-93. According to the Brunauer–Deming–Deming–Teller (BDDT) classification, the N_2 isotherms of the two resins belonged to type-IV. The A-IRA-93 and mA-IRA-93 resins have some micropores, and this conclusion was deduced from the not increased N_2 capacity at a very low relative pressure (P/P_0 < 0.05 micropores), the hysteresis loop at a medium relative pressure (0.05 < P/P_0 < 0.9 mesopores) and the further increased N_2 capacity at a higher relative pressure (P/P_0 > 0.95, macropores) [37].

3.2. Effect of pH

Extraction of uranyl ions by the A-IRA-93 and the mA-IRA-93 resins from acetate medium was studied in the pH range from 2.0 to 7.0. The study outcomes are shown in Fig. 5.

From Fig. 5 it is observed that the two resins have the same trend overall the uranyl ions sorption. We also

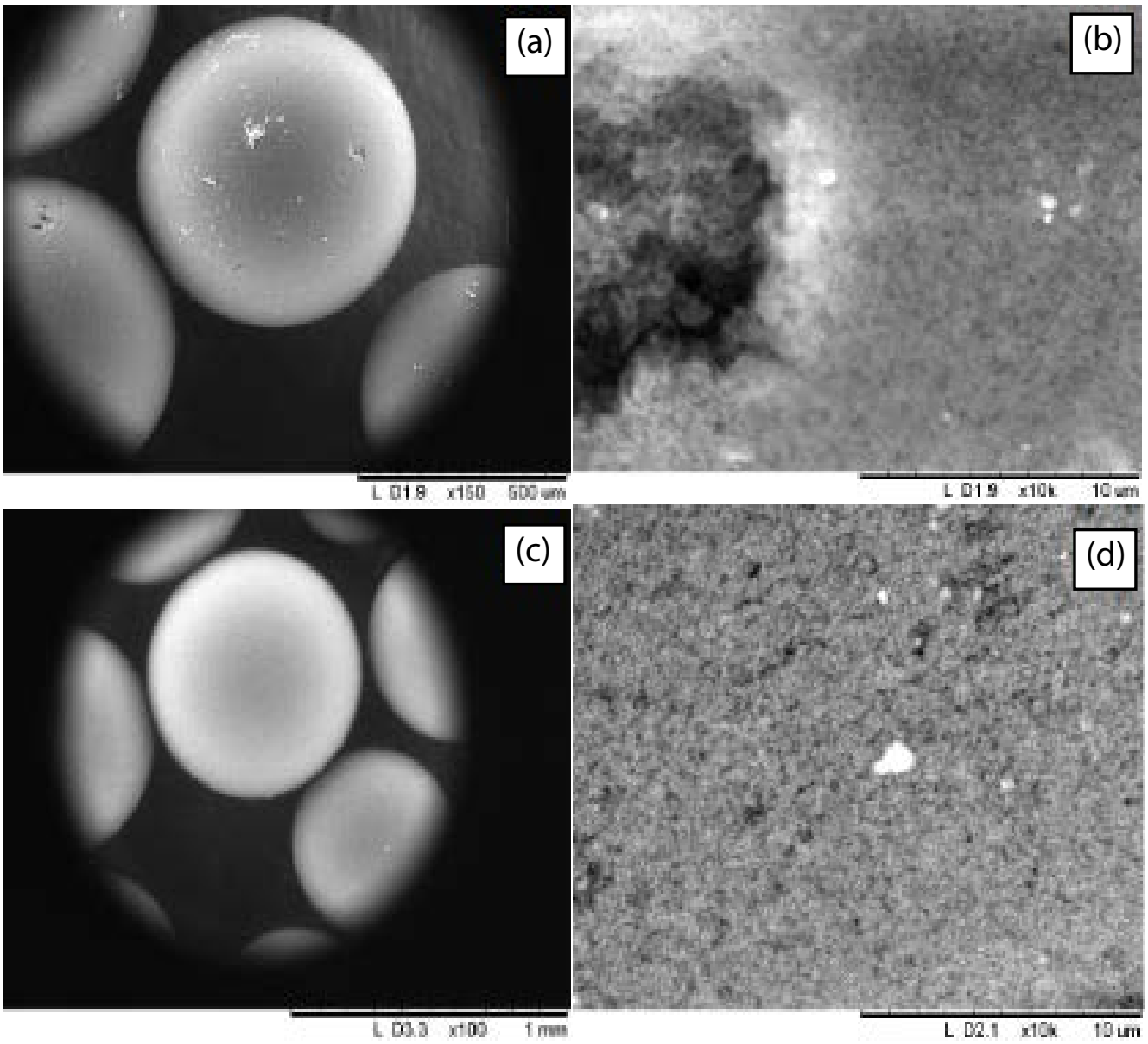

Fig. 2. SEM images of the A-IRA-93 (a, b) and mA-IRA-93 resins (c, d).

Table 1
Textural and structural parameters of the A-IRA-93 and mA-IRA-93 resins

Adsorbent	BET surface area ($m^2\ g^{-1}$)	Pore volume ($cm^3\ g^{-1}$)	Barrett–Joyner–Halenda pore size (nm)	Micropore surface area ($m^2\ g^{-1}$)	d_{110} (Å)	a (Å)
A-IRA-93	37.3022	0.318665	35.3815	36.0261	4.91	9.82
mA-IRA-93	33.2794	0.366068	45.5060	32.1775	4.07	8.14

observed that the retention of uranyl ions on the resin increases with the pH from 2.0 to 3.5, and then the extraction yield decreases with pH increase up to pH = 7. It can be seen that maximal uranium extraction yields obtained at an initial pH of 3.5 were 85.8% and 82.8% for mA-IRA-93 then A-IRA-93 respectively. This could be due to the presence of $UO_2(CH_3COO)^+$, $(UO_2)_2(OH)_2^{2+}$ and $UO_2(OH)^+$ which are in equilibrium with the UO_2^{2+}. The complexes formed between $UO_2^{2+}(CH_3COO)^+$ and $(UO_2)_2(OH)_2^{2+}$ and functional group are more stable (Fig. 6) [38].

At higher pH (3.5 < pH < 7.0), UO_2^{2+} uptake decreased slowly, this can be due to the presence of different more

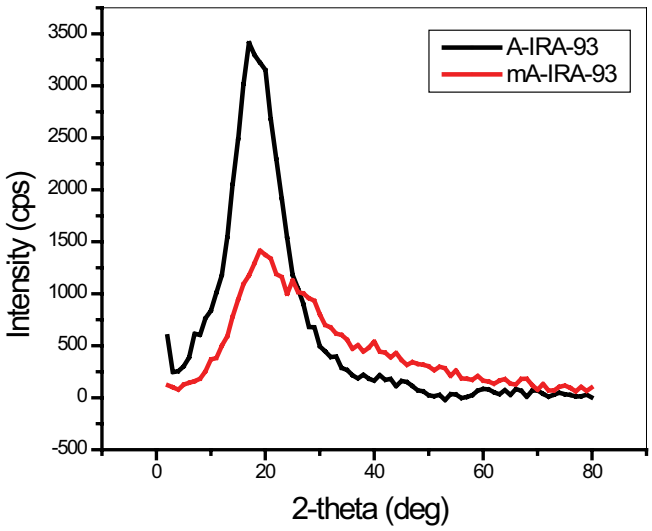

Fig. 3. Low angle XRD pattern of the A-IRA-93 and mA-IRA-93 resins.

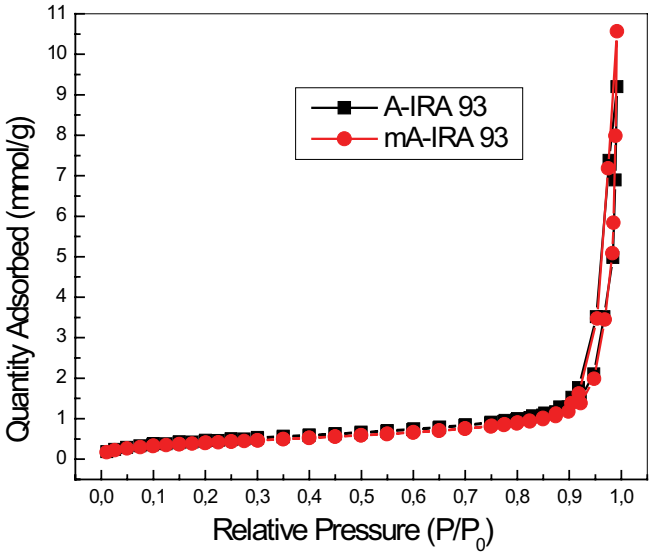

Fig. 4. N_2 adsorption–desorption isotherms (measured at 77 K, the outgas in temperature was 423 K, and the duration time was 8 h).

stable and soluble U(VI) hydrolysis species such as $UO_2(OH)^+$ and $(UO_2)_2(OH)_2^{2+}$ (shown in Fig. 7). These species are more difficult to adsorb [39]. To achieve a higher adsorption capacity, the following adsorption studies were carried out at $pH_i = 3.5$.

3.3. Effect of contact time

To study the effect of contact time, we have obtained the extraction yields at different times and different weights of resins (Fig. 8). It is seen that the extraction yield of uranyl ions on A-IRA-93 resin increases over time, for the three resin masses tested. Equilibrium is reached after 60 min of stirring. The uranyl ions sorption

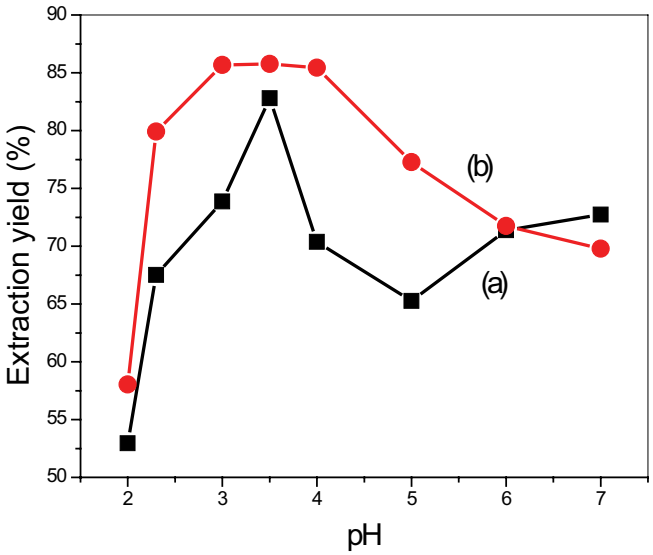

Fig. 5. Removal of uranyl ions by A-IRA-93 (a) and mA-IRA-93 (b) resins, as a function of initial pH. $[UO_2^{2+}] = 10^{-4}$ mol L^{-1}, w(A-IRA-93) = 0.03 g, w(mA-IRA-93) = 0.02 g, V = 4 mL, Ø = 250 rpm, T = 22°C ± 1°C, and t_e = 60 min.

capacities for the three masses, w = 0.020, 0.025 and 0.030 g of resin were q_e = 5.60, 3.95 and 3.76 mg g^{-1}, respectively. However, for mA-IRA-93, we observe that the extraction efficiency increases rapidly with increasing time. The time needed for mA-IRA-93 to adsorb the maximum of uranyl was 30 min and the UO_2^{2+} ion sorption capacities for the three masses w = 0.020, 0.1 and 0.2 g of resin are q_e = 8.09, 1.66 and 0.74 mg g^{-1}, respectively. Thus, extraction with mA-IRA-93 was more efficient than with A-IRA-93; the time of extraction was smaller (30/60 min).

Therefore, for the same mass used w = 0.02 g for the two resins, the mA-IRA-93 will give better results for the extraction of UO_2^{2+}.

3.4. Adsorption kinetics

Kinetics of sorption describing the solute uptake rate, which, in turn, governs the residence time of the sorption reaction, is one of the important characteristics defining the efficiency of sorption [37]. The linear form of the pseudo-first-order rate equation is expressed as Eq. (4):

$$\ln(q_e - q_t) = \ln q_e - k_1 \cdot t \tag{4}$$

The linear form of the pseudo-second-order rate equation is given as [36],

$$\frac{t}{q_t} = \frac{1}{q_e^2} + \frac{t}{q_e} \tag{5}$$

where q_e and q_t are the amounts of sorbed UO_2^{2+} on the two resins A-IRA-93 and mA-IRA-93 at equilibrium and at time t, respectively (mg g^{-1}), k_1 is the first-order adsorption rate constant (min^{-1}), k_2 is the pseudo-second-order adsorption rate constant (g mg^{-1} min^{-1}).

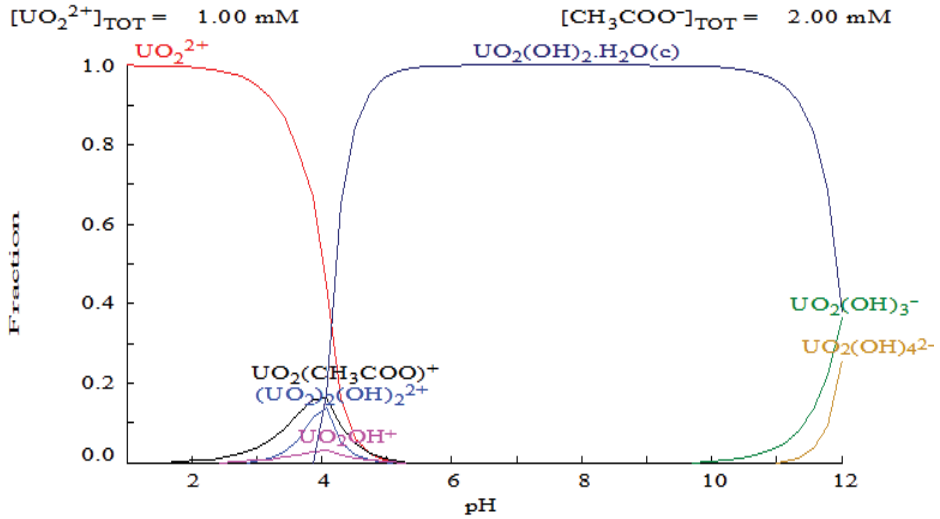

Fig. 6. Diagram of the predominence of the uranyl species in aqueous phase given by MEDUSA, $[UO_2^{2+}] = 10^{-3}$ mol L^{-1}, $1 \le pH \le 12$ [33].

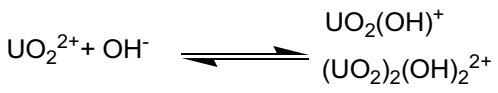

Fig. 7. U(VI) hydrolysis species.

The correlation coefficients (R^2) for the pseudo-first-order equation and the theoretical q_e values were calculated from the pseudo-first-order equation are not in agreement with the experimental data (Table 1), suggesting that this adsorption system is not a pseudo-first-order reaction. High correlation coefficients are obtained when employing the pseudo-second-order model and the calculated equilibrium sorption capacities were similar to the experimental data (Table 2). This indicates that the pseudo-second-order model can be applied to predict the adsorption kinetic (Fig. 9).

3.5. Diffusion study

The uranyl ions transport from the solution phase to the surface of the A-IRA-93 and the mA-IRA-93 resins occurs in several steps [40,41], (i) the diffusion of ions from the solution to the A-IRA-93 and the mA-IRA-93 surfaces, (ii) the diffusion of ions within the solid resin and (iii) the chemical reactions between ions and functional groups of the resins. The adsorption of the metal is governed by the slowest of these processes.

If the liquid film diffusion controls the rate of exchange, Eq. (6) can be used.

$$-\ln(1-F) = k \cdot t \tag{6}$$

where F is the fractional attainment of equilibrium, which is expressed as $F = q_t/q_e$ [41], q_e and q_t are the amounts of sorbed

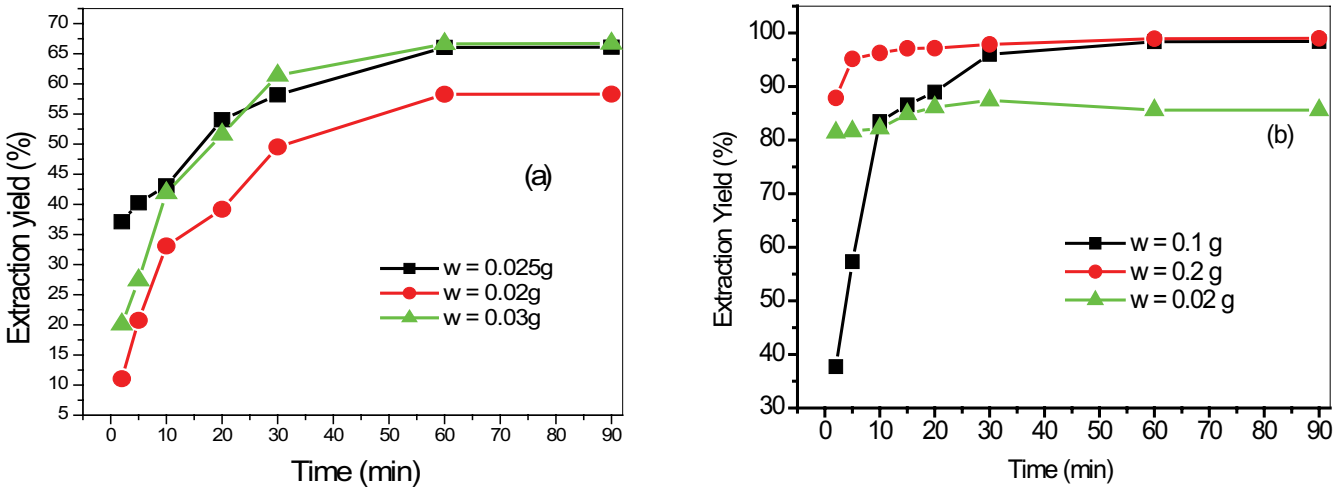

Fig. 8. Removal of uranyl by A-IRA-93 resin (a), mA-IRA-93 resin (b) as a function of time with three different weights of resins. $[UO_2^{2+}] = 10^{-4}$ mol L^{-1}, pH = 3.5, V = 4 mL, Ø = 250 rpm, and T = 22°C ± 1°C.

Table 2
Comparison of the pseudo-first-order and pseudo-second-order models for the adsorption of uranyl

Adsorbent	w, g	$q_{e(exp)}$, mg g^{-1}	Pseudo-first-order model	Pseudo-second-order model
A-IRA-93	0.02	5.6023	$q_{e(cal)}$ = 2.2512 mg g^{-1} k_1 = 0.0395 min^{-1} R^2 = 0.77	$q_{e(cal)}$ = 5.8061 mg g^{-1} k_2 = 0.0468 g mg^{-1} min^{-1} R^2 = 0.99
	0.025	3.9540	$q_{e(cal)}$ = 3.4179 mg g^{-1} k_1 = 0.0563 min^{-1} R^2 = 0.97	$q_{e(cal)}$ = 4.6720 mg g^{-1} k_2 = 0.0181 g mg^{-1} min^{-1} R^2 = 0.99
	0.03	3.7689	$q_{e(cal)}$ = 3.1783 mg g^{-1} k_1 = 0.0754 min^{-1} R^2 = 0.98	$q_{e(cal)}$ = 4.2290 mg g^{-1} k_2 = 0.0316 g mg^{-1} min^{-1} R^2 = 0.99
mA-IRA-93	0.02	8.3439	$q_{e(cal)}$ = 5.2493 mg g^{-1} k_1 = 0.1029 min^{-1} R^2 = 0.96	$q_{e(cal)}$ = 8.8448 mg g^{-1} k_2 = 0.0343 g mg^{-1} min^{-1} R^2 = 0.99
	0.10	1.6782	$q_{e(cal)}$ = 0.1197 mg g^{-1} k_1 = 0.0711 min^{-1} R^2 = 0.79	$q_{e(cal)}$ = 1.6845 mg g^{-1} k_2 = 1.9866 g mg^{-1} min^{-1} R^2 = 0.99
	0.20	0.7414	$q_{e(cal)}$ = 0.0475 mg g^{-1} k_1 = 0.0271 min^{-1} R^2 = 0.71	$q_{e(cal)}$ = 0.7330 mg g^{-1} k_2 = 6.8712 g mg^{-1} min^{-1} R^2 = 0.99

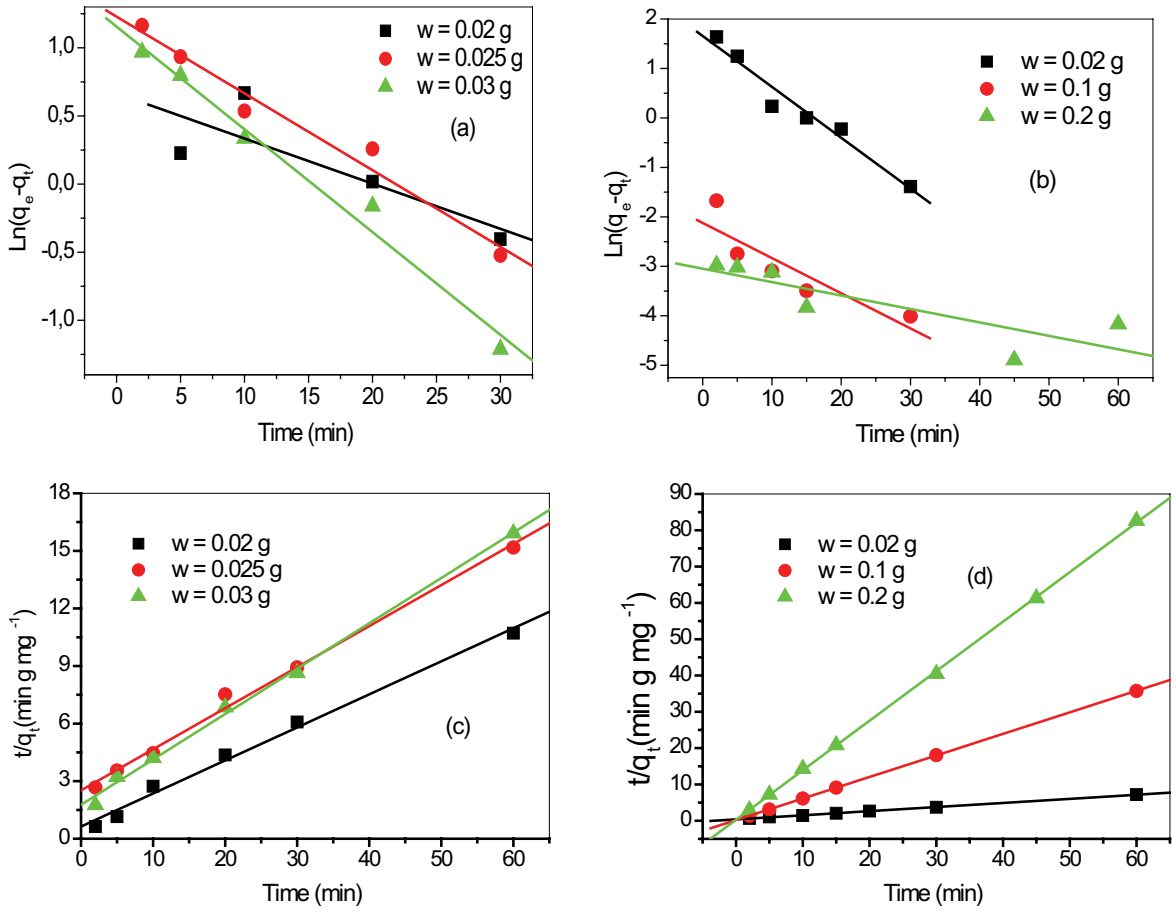

Fig. 9. Pseudo-first-order and pseudo-second-order plots of UO_2^{2+} adsorption kinetics onto: A-IRA-93 resin (a, c), respectively and mA-IRA-93 resin (b, d), respectively, as a function with three different weights of resins. [UO_2^{2+}] = 10^{-4} mol L^{-1}, pH = 3.5, V = 4 mL, Ø = 250 rpm, and T = 22°C ± 1°C.

UO_2^{2+} on the two resins A-IRA-93 and mA-IRA-93 at equilibrium and at time t, respectively (mg g^{-1}).

In the case of diffusion of ions in the A-IRA-93 and the mA-IRA-93 resins phase controlling process, the relation used is Eq. (7) [41].

$$-\ln\left(1-F^2\right)=k\cdot t \tag{7}$$

In both Eqs. (6) and (7), k is the kinetic coefficient or rate constant which is defined by Eq. (8) [41].

$$k=\frac{D_r\cdot\pi^2}{r_0^2} \tag{8}$$

where D_r is the diffusion coefficient in the A-IRA-93 and the mA-IRA-93 phases and r_0 is the average radius of A-IRA-93 and the mA-IRA-93 resins (0.3 mm).

When the adsorption of metal ion involves mass transfer accompanied by chemical reaction the process can be explained by the moving boundary model [41]. This model assumes a sharp boundary that separates a completely reacted shell from an unreacted core and that advances from the surface toward the center of the solid with the progression of adsorption. In this case, the rate equation is given by Eq. (9) [41].

$$3-3\left(1-F\right)^{2/3}-2F=k\cdot t \tag{9}$$

After testing both mathematical models proposed above, diffusion analysis was adequate with the particle model diffusion for mA-IRA-93, however, adsorption can be explained by chemical reaction model for A-IRA-93, with good correlation coefficients at initial adsorption ($t \le 30$ min) (Fig. 10; Table 3). For the present system, the value of D_r, fall well within the values reported in literature, especially for chemisorptions system (10^{-9}–10^{-17} m^2 s^{-1}) [42].

3.6. Effect of initial metal concentration

The extraction equilibrium of uranyl ions between aqueous solution and resins can be described by a sorption isotherm. The extraction experiments were performed using different initial concentration of UO_2^{2+} at T = 22°C ± 1°C. Sorption of uranyl ions on A-IRA-93 and mA-IRA-93 resins were presented in Fig. 11 in term of extraction yield as a function of the initial uranyl ions concentration in the aqueous medium.

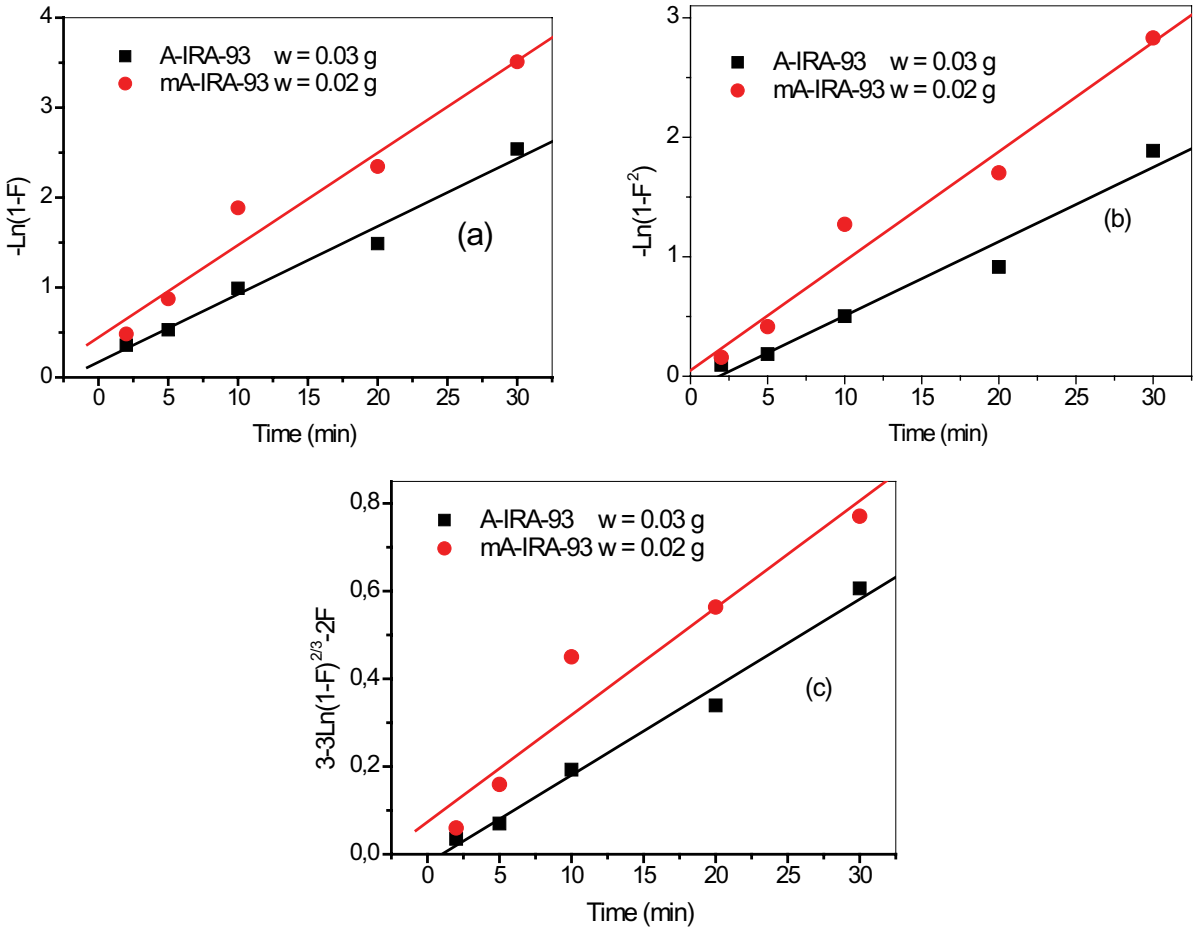

Fig. 10. Plots of diffusion study for UO_2^{2+} sorption on A-IRA-93 and mA-IRA-93 resins at different time. $[UO_2^{2+}]_0 = 10^{-4}$ mol L^{-1}, V = 4 mL, Ø = 250 rpm, and T = 22°C ± 1°C. Film diffusion (a), particle diffusion (b), and chemical reaction (c).

Table 3
Kinetic and diffusion parameters of uranyl onto A-IRA-93 and mA-IRA-93 resins

Adsorbent	Film diffusion, Eq. (6)	Particle diffusion, Eq. (7)	Chemical reaction, Eq. (9)
A-IRA-93	$k = 0.07544\ min^{-1}$	$k = 0.06213\ min^{-1}$	$k = 0.02005\ min^{-1}$
$w = 0.03$ g	$R^2 = 0.99$	$R^2 = 0.98$	$R^2 = 0.99$
		$D_r = 5.6713 \times 10^{-10}\ m^2\ min^{-1}$	$D_r = 1.8302 \times 10^{-9}\ m^2\ min^{-1}$
mA-IRA-93	$k = 0.1029\ min^{-1}$	$k = 0.09168\ min^{-1}$	$k = 0.02458\ min^{-1}$
$w = 0.02$ g	$R^2 = 0.98$	$R^2 = 0.98$	$R^2 = 0.96$
		$D_r = 8.3687 \times 10^{-10}\ m^2\ min^{-1}$	$D_r = 2.2437 \times 10^{-10}\ m^2\ min^{-1}$

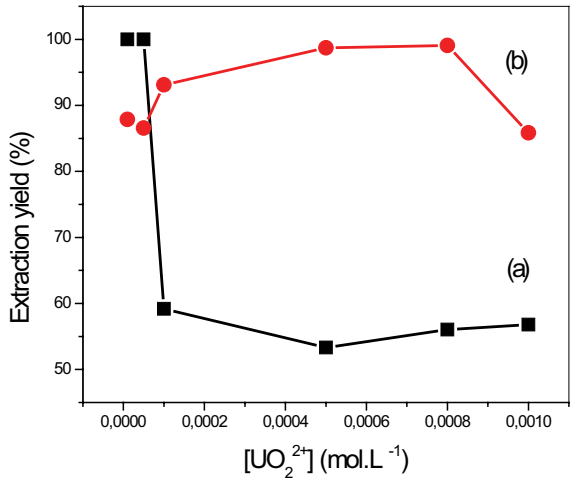

Fig. 11. Extraction of uranyl ions by: (a) A-IRA-93 and (b) mA-IRA-93 resins as a function of initial UO_2^{2+} concentration. pH = 3.5, w(A-IRA-93) = 0.03 g, w(mA-IRA-93) = 0.02 g, V = 4 mL, Ø = 250 rpm, T = 22°C ± 1°C and t_e = 60 min.

The data indicates that the initial metal concentration determines the equilibrium concentration, and also determines the uptake rate of metal ion and the kinetic character of the process for both resins.

In the case mA-IRA-93 resin, at low concentrations, the ratio of the initial number of moles of UO_2^{2+} ion to the available surface area of resin is larger and subsequently, the fractional ion exchange becomes independent of initial concentrations. The rapid metal extraction has significant practical importance, as this will facilitates with the small amount of resins to ensure efficiency and economy.

The amount of UO_2^{2+} ions adsorbed per unit mass of the mA-IRA-93 resin increased with the initial metal concentration as expected. This is due to the fact that sorption sites took up the available metal ions more quickly at low concentration, but metal needed to diffuse to the inner sites of the sorbent for high concentration. The extraction yield of uranyl sorption was 98% at $[UO_2^{2+}] = 8.\ 10^{-4}$ mol L^{-1}. The initial rate of sorption was greater for higher initial uranyl concentrations, because the resistance to the metal uptake decreased as the mass transfer driving force increased.

It is also noticed that an increase in the initial uranyl concentration leads to a decrease in the metal removal.

This can be explained as follows: at low metal/sorbent ratios, there are a number of sorption sites in mA-IRA-93 structure. As the metal/sorbent ratio increases, sorption sites are saturated, resulting in decreases in the sorption efficiency.

For A-IRA-93 resin, at low concentrations, the extraction yield of uranyl sorption is 100% for initial concentrations (1.10^{-5}–5×10^{-5} mol L^{-1}). This can be explained that by a total sorption.

For higher initial uranyl concentrations (1.10^{-4}–1.10^{-3} mol L^{-1}), the graph seems to be constant at around 58%.

3.7. Isotherm adsorption

The sorption data (Fig. 12), commonly known as adsorption isotherms, are basic requirements for the design of adsorption systems. Adsorption models, Langmuir [Eq. (10)] and Freundlich [Eq. (11)], were used to describe the equilibrium between adsorbed UO_2^{2+} ions on the A-IRA-93 resin and the mA-IRA-93 resin sites [41]. For the interpretation of the two models, we have used the following equations [43].

$$\frac{C_e}{q_e} = \frac{C_e}{q_m} + \frac{1}{\left(q_m \cdot K_L\right)} \tag{10}$$

$$\ln q_e = \ln K_F + n \cdot \ln C_e \tag{11}$$

where C_e is the equilibrium concentration of uranyl (mg L^{-1}), q_e is the amount of uranyl ions sorbed on the A-IRA-93 resin and mA-IRA-93 resin (mg g^{-1}), K_L is the Langmuir adsorption constant (L mg), q_m is the maximum amount of uranyl ions that can be sorbed (mg g^{-1}), K_F is the Freundlich adsorption constant (g^{-1}), and n is a constant that indicates the capacity and intensity of the adsorption process, respectively.

The Sips isotherm is a combined form of Langmuir and Freundlich models [19]. When approaches a low value, the Sips isotherm effectively reduces to Freundlich, while at high, it predicts the Langmuir monolayer sorption characteristic. The model can be written as [19]:

$$q_e = \frac{q_{ms} K_S C_e^{1/n}}{1 + K_S C_e^{1/n}} \tag{12}$$

The Sips linear equation model is expressed as:

$$\frac{1}{q_e} = \frac{1}{q_{ms} \cdot K_S} \cdot \frac{1}{C_e^{1/n}} + \frac{1}{q_{ms}} \tag{13}$$

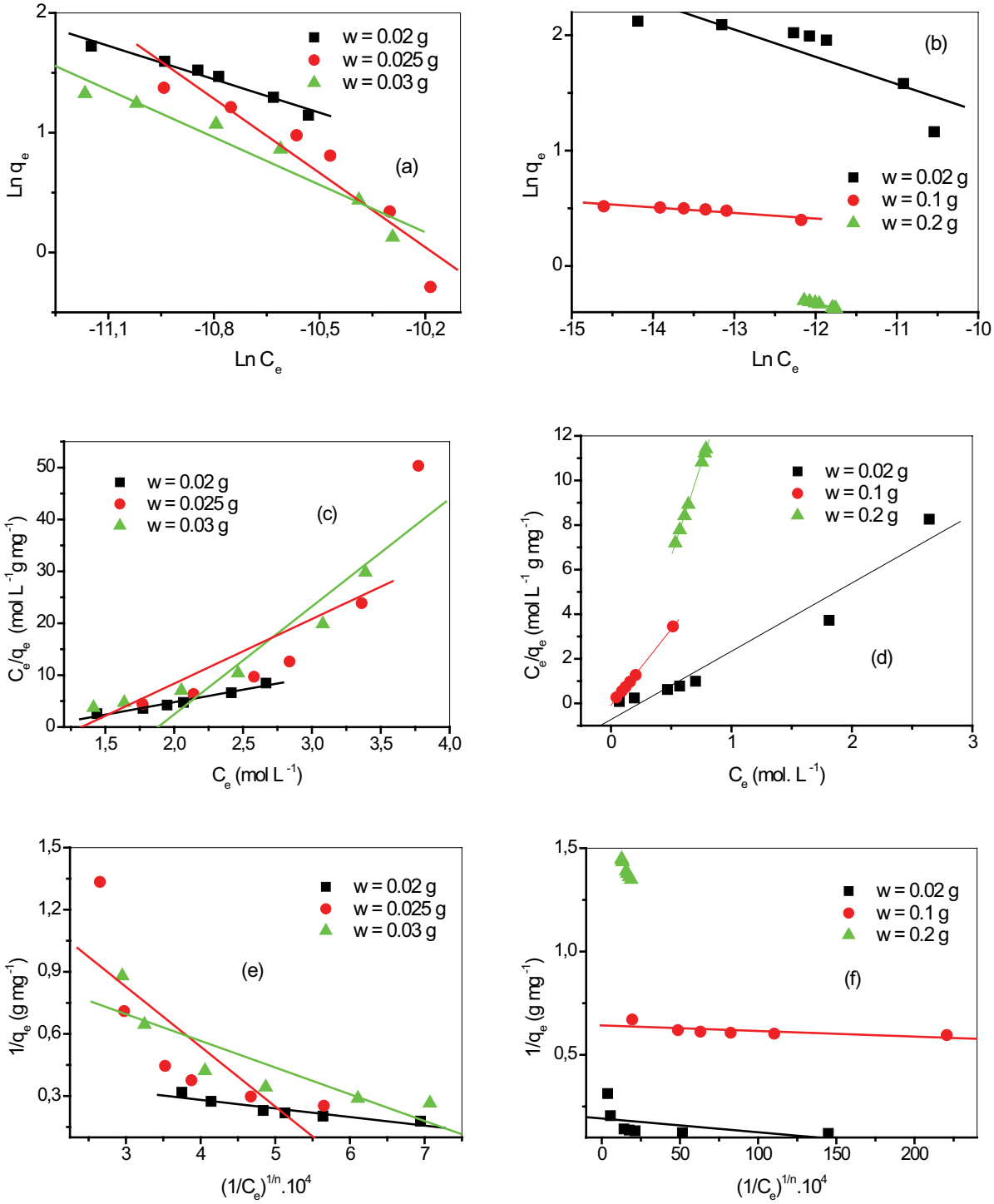

Fig. 12. Freundlich, Langmuir and Sips isotherms plots for the sorption of uranyl onto: A-IRA-93 resin (a, c, e), respectively and mA-IRA-93 resin (b, d, f) respectively, with three different weights of resins.

where q_{ms} (mg g^{-1}) is the Sips maximum adsorption capacity, K_S (g^{-1}) is the Sips model isotherm constant, and $1/n$ is the Sips model exponent.

We concluded from the best correlation coefficients (Table 4) that the Freundlich equation fits the data better than the Langmuir model for the A-IRA-93 resin indicating a multilayer adsorption nature of this metal ions on this resin [44].

The Langmuir model indicates that the removal of UO_2^{2+} ions is uniformly distributed in a monolayer coverage at the surface of the sorbent [45]. It is noteworthy that the mA-IRA-93 shows significantly similar extraction capacities,

towards UO_2^{2+} ions as compared with other materials as seen in Table 5.

3.8. Effect of ionic strength

The influences of sodium salts on uranyl extraction were studied at varying concentrations of NaCl and CH_3COONa in the ranges of (0–1 mol L^{-1}). Figs. 13 and 14 show that, for mA-IRA-93, it can be seen that the addition of the CH_3COONa salt influences the uranyl extraction yield (from 96.3% to 81.4%) for a salt concentration interval (from 0 to 1 mol L^{-1}). NaCl salt also affects the extraction yield (from 98.3% to 79.95%) for a salt concentration interval (from 0 to 0.8 mol L^{-1}). This can however be explained as the result of an electrostatic competition of Na^+ at higher concentrations, with UO_2^{2+}. Since deprotonated P–OH groups on mA-IRA-93 are negatively charged, they will electrostatically attract any cation. So, for high ionic strengths, adsorption sites will be surrounded by counter ions and they partially lose their charge, this weakens the binding force due to electrostatic interaction [41]. For A-IRA-93, it can be seen that the addition of the CH_3COONa salt slightly influences the uranyl extraction yield (from 91.9% to 83.0%) for a salt concentration interval (from 0.3 to 1.0 mol L^{-1}). This result can be explained also by a slight competition between the UO_2^{2+} and Na^+ cations on the active sites of the Amberlite IRA-93 resin. However, the NaCl salt has not an influence on the extraction efficiency of UO_2^{2+} ions.

3.9. Thermodynamic parameters

The effect of temperature on the removal of uranyl ions from acetate solution by A-IRA-93 resin and mA-IRA-93

Table 4
Comparison of isotherm models parameters for the adsorption of UO_2^{2+} on A-IRA-93 resin and mA-IRA-93 resin

Adsorbent	w, g	Freundlich isotherm	Langmuir isotherm	Sips isotherm
A-IRA-93	0.02	$1/n$ = –0.92986 $K_F = 1.84 \times 10^{-4}$ g^{-1} R^2 = 0.97	q_m = 2.0819 mg g^{-1} K_L = –99795.86 L mg^{-1} R^2 = 0.97	q_{ms} = 2.2368 mg g^{-1} K_S = –10.79 L mg^{-1} R^2 = 0.87 $1/n$ = 0.5814
	0.025	$1/n$ = –2.06608 $K_F = 7.35 \times 10^{-10}$ g^{-1} R^2 = 0.89	q_m = 0.4811 mg g^{-1} K_L = –53139.29 L mg^{-1} R^2 = 0.81	q_{ms} = 0.5899 mg g^{-1} K_S = –5.86 L mg^{-1} R^2 = 0.63 $1/n$ = 0.4556
	0.03	$1/n$ = –1.32139 $K_F = 1.65 \times 10^{-6}$ g^{-1} R^2 = 0.93	q_m = 0.8039 mg g^{-1} K_L = –75400.10 L mg^{-1} R^2 = 0.91	q_{ms} = 0.9235 mg g^{-1} K_S = –8.39 L mg^{-1} R^2 = 0.75 $1/n$ = 0.5673
mA-IRA-93	0.02	$1/n$ = –0.2363 K_F = 0.35 g^{-1} R^2 = 0.71	q_m = 3.2638 mg g^{-1} $K_L = -4.2190 \times 10^5$ L mg^{-1} R^2 = 0.95	q_{ms} = 5.2070 mg g^{-1} K_S = –288.19 L mg^{-1} R^2 = 0.23 $1/n$ = 7.6377
	0.10	$1/n$ = –0.0484 K_F = 0.84 g^{-1} R^2 = 0.86	q_m = 1.4637 mg g^{-1} $K_L = -8.0082 \times 10^6$ L mg^{-1} R^2 = 0.99	q_{ms} = 1.5562 mg g^{-1} K_S = –2367.71 L mg^{-1} R^2 = 0.50 $1/n$ = 11.7840
	0.20	$1/n$ = –0.1851 K_F = 0.08 g^{-1} R^2 = 0.99	q_m = 0.6011 mg g^{-1} $K_L = -9.6593 \times 10^5$ L mg^{-1} R^2 = 0.99	q_{ms} = 0.6030 mg g^{-1} K_S = –98.30 L mg^{-1} R^2 = 0.99 $1/n$ = 1.5114

Table 5
Comparison of uranyl removal capacities of the mA-IRA-93 with other sorbents

Materials	$C_0 \times 10^4$ mol L^{-1}	pH	w, g	Contact time, min	Capacity, mg g^{-1}	References
Lewatit TP 260	0.3	4.1	0.060	120	58.33	[45]
PVA with functionalized with vinylphosphonic acid (PVA-VPA)	2.5	4.5	0.300	30	32.10	[38]
Phosphonic acid-imbedded polyurethane foam mA-IRA-93	0.24	7.0	0.200	5 h	0.825	[46,47]
	1.0	3.5	0.020	60	8.34	This work

resin at pH = 3.5, V = 4 mL, w = 0.03 g and w = 0.02 g for A-IRA-93 and mA-IRA-93 resins respectively, Ø = 250 rpm and concentration of $[UO_2^{2+}] = 10^{-4}$ mol L^{-1} was studied for the determination of thermodynamic data such as, the Gibbs free energy change (ΔG), enthalpy change (ΔH) and entropy change (ΔS). ΔG was calculated using the following equations [40]:

$$\Delta G = \Delta H - T \cdot \Delta S \quad (14)$$

$$\Delta G = -RT \cdot \ln K_D \quad (15)$$

where R is the gas constant (8.314 J mol^{-1} K^{-1}) and T the temperature (K).

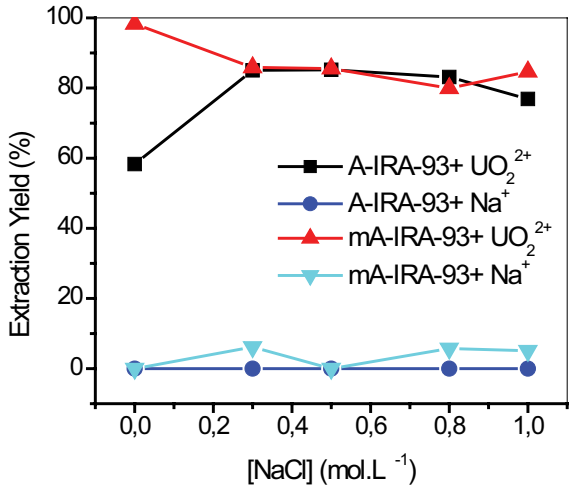

Fig. 13. Removal of uranyl and sodium by A-IRA-93 and mA-IRA-93 resins as a function of initial concentration of NaCl. $[UO_2^{2+}] = 10^{-4}$ M, pH = 3.5, w(A-IRA-93) = 0.03 g, w(mA-IRA-93) = 0.02 g, V = 4 mL, Ø = 250 rpm, T = 22°C ± 1°C and t_e = 60 min.

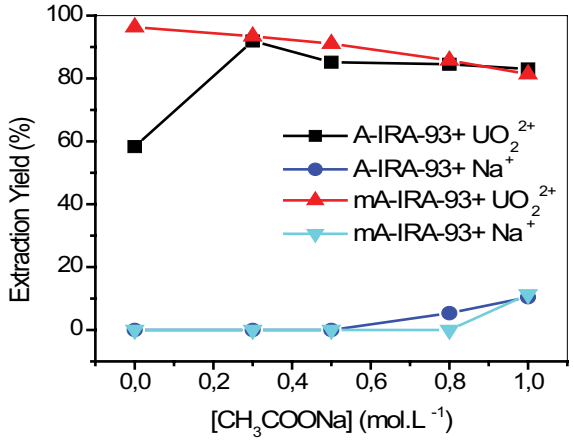

Fig. 14. Removal of uranyl and sodium by A-IRA-93 and mA-IRA-93 resins as a function of initial concentration of CH_3COONa. $[UO_2^{2+}] = 10^{-4}$ M, pH = 3.5, w(A-IRA-93) = 0.03 g, w(mA-IRA-93) = 0.02 g, V = 4 mL, Ø = 250 rpm, T = 22°C ± 1°C and t_e = 60 min.

The relation between K_D, ΔH and ΔS can be described by Van't Hoff correlation in Eq. (18).

$$\ln K_D = \frac{\Delta S}{R} - \frac{\Delta H}{RT} \quad (16)$$

Fig. 15 shows the removal yield of uranyl ions onto A-IRA-93 and its modified form resins as a function of the temperature. It can be seen that the extraction yield of uranyl increases with increasing temperature, this attitude indicates that uranyl sorption on both resins is an endothermic and spontaneous process, as supported by the positive values of ΔH and ΔS (Fig. 16 and Table 6), the decrease in ΔG values with increase in temperature showed that the sorption was most favorable at higher temperature.

$\Delta G < 0$ indicated that the sorption process of uranyl was spontaneous for the two resins. The ratio $\Delta G_{mA\text{-}IRA\text{-}93}/\Delta G_{A\text{-}IRA\text{-}93}$ = 10.58 show that the extraction by the mA-IRA-93 is more spontaneous than the extraction by the A-IRA-93.

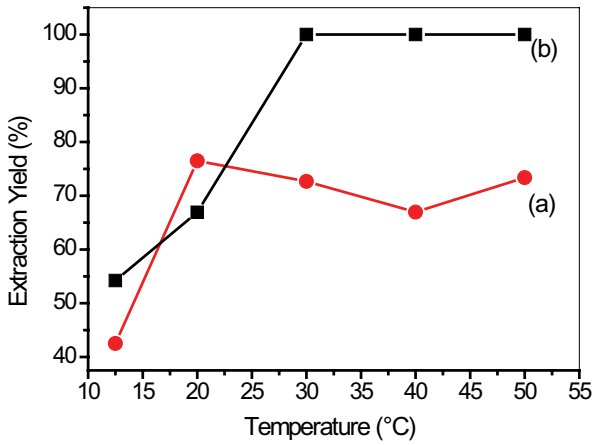

Fig. 15. Removal of uranyl by: (a) A-IRA-93 and (b) mA-IRA-93 resins as a function of temperature, pH = 3.5, $[UO_2^{2+}] = 10^{-4}$ mol L^{-1}, w(A-IRA-93) = 0.03 g, w(mA-IRA-93) = 0.02 g, V = 4 mL, Ø = 250 rpm, and t_e = 60 min.

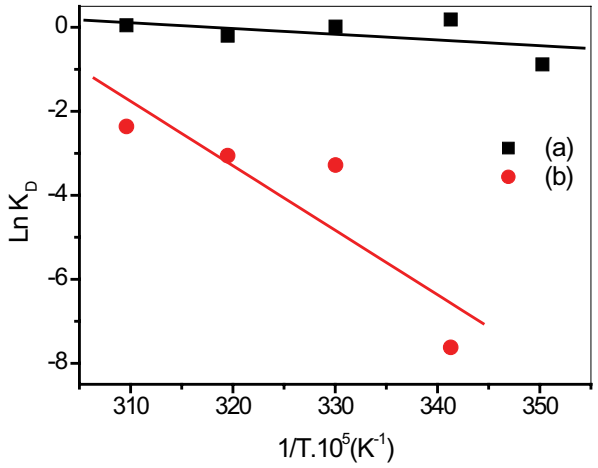

Fig. 16. Plot of Eq.14 for the uranyl sorption on (a) A-IRA-93 and (b) mA-IRA-93 resins.

Table 6
Thermodynamic parameters for the removal of UO_2^{2+} on A-IRA-93 and mA-IRA-93 resins

Material	ΔH (kJ mol^{-1})	ΔS (J mol^{-1} K^{-1})	ΔG (kJ mol^{-1}) at 295°K
A-IRA-93	0.11331×10^{-3}	36.0243	–10.6270
mA-IRA-93	1.2769×10^{-3}	381.2271	–112.4607

3.10. Fractional experimental design $3^{(3-1)}$

A fractional factorial design $3^{(3-1)}$ is proposed. It is built from 9 tests. It was defined by the design matrix shown in Table 7.

Furthermore, the study of such a system was based on the analysis of variances which expresses the importance of the influence of each of the factors (X_1, X_2 and X_3) on the response (Y). This analysis adopts the quadratic mathematical model described by Eq. (17):

$$Y = a_0 + \sum a_i \cdot X_i + \sum b_i \cdot X_i^2 \quad (17)$$

where a_0 is the average yield of the extraction; a_i and b_i represent the coefficients of the model.

Table 7
Design matrix for a $3^{(3-1)}$ fractional factorial experiment

N° experiment	X_1	X_2	X_3	Response (Y) %
1	–1	–1	–1	Y_1
2	–1	0	+1	Y_2
3	–1	+1	0	Y_3
4	0	–1	+1	Y_4
5	0	0	0	Y_5
6	0	+1	–1	Y_6
7	+1	–1	0	Y_7
8	+1	0	–1	Y_8
9	+1	+1	+1	Y_9

3.11. Factors and areas of study

Preparing for the experiment involves first looking for all the factors that can influence the process being studied, and then the areas of study for each of these factors. Therefore, the parameters which seem to be dominant are:

- Mass of the mA-IRA-93,
- Molar concentration of the metal [UO_2^{2+}],
- Molar concentration of sodium acetate (CH_3COONa).

In addition, each of them is studied in its own domain of influence as indicated in Table 8. In addition, it is imperative to note that all the experiments of this plan are carried out at:

- T = 22°C ± 1°C;
- pH_i = 3.5 ;
- Mechanical agitation of 250 rpm.

Table 8
Selected parameters and field of study

Parameter	Designation	Range studied
Mass of mA-IRA-93, (g)	Q	0.01–0.05
[UO_2^{2+}], (M)	C	10^{-5}–10^{-3}
[CH_3COONa], (M)	S	0.2–1.0

3.12. Establishment of the mathematical model

The extraction of uranyl ions by mA-IRA-93 was studied using the test matrix shown in Table 9. Statistical studies are carried out using the STATISTICA 12 software which is suitable for the resolution of fractional plans, type $3^{(3-1)}$ [48].

The lowest yield was 25.3%. It was obtained with 0.01 g of mA-IRA-93, a concentration equal to 0.6 M of CH_3COONa and a concentration of 10^{-3} M of UO_2^{2+}.

- Best yield was 100% and it was observed on experiment 9.
- Mean extraction yield was around 65.3%.

Therefore, the results were translated into mathematical polynomials using variance analysis (ANOVA). The results are shown in Table 10.

4. Conclusions

A novel method was proposed to synthesize a new sorbent the di(methylenephosphonic) acid grafted on Amberlite IRA 93 resin using the Moedrizer-Irani reaction and was used subsequently as support material for UO_2^{2+} ions sorption. The extraction yield was determined as a function of various parameters such as extraction time, initial pH, uranyl concentration, temperature and ionic strength. The maximal experimental capacities obtained were 3.77 mg g^{-1} for A-IRA-93 resin and 8.34 mg g^{-1} for mA-IRA-93 resin. Modification of the resin increases the retention capacity by a factor of 2.21. The removal of uranyl achieves equilibration at 30 and 60 min for mA-IRA-93 resin and A-IRA-93 resin, respectively. Optimal extraction yield was achieved for an initial pH equal at 3.5 for the two resins.

The kinetics of uranyl sorption on the two resins follows the pseudo-second-order model. The equilibrium isotherm for sorption of the investigated metal ions has been modeled successfully using the Freundlich isotherm for A-IRA-93 resin and Langmuir isotherm for mA-IRA-93 resin. Diffusion models indicated that particle diffusion model was adequate for mA-IRA-93 resin; however, adsorption can be explained by chemical reaction model for A-IRA-93 resin. Thermodynamics data leads to endothermic process for the sorption of UO_2^{2+} ions on the two resins. Thermodynamic study has shown also a negative

Table 9
Parameter values and their responses when extracting UO_2^{2+}

N° experiment	Parameters			Reduced variables			Response
	mA-IRA-93, (g)	$[UO_2^{2+}]$, (M)	$[CH_3COONa]$, (M)	X_1	X_2	X_3	Extraction yield, Y (%)
1	0.01	10^{-5}	0.2	–1	–1	–1	100
2	0.01	10^{-4}	1.0	–1	0	+1	44.0
3	0.01	10^{-3}	0.6	–1	+1	0	25.3
4	0.03	10^{-5}	1.0	0	–1	+1	100
5	0.03	10^{-4}	0.6	0	0	0	65.3
6	0.03	10^{-3}	0.2	0	+1	–1	31.7
7	0.05	10^{-5}	0.6	+1	–1	0	84.0
8	0.05	10^{-4}	0.2	+1	0	–1	74.4
9	0.05	10^{-3}	1.0	+1	+1	+1	42

Table 10
Mathematical models of extraction of UO_2^{2+} by mA-IRA-93

Mathematical model in reduced coordinates	
$Y(\%) = 63.3 + 3.67X_1 - 20.78X_2 - 2.25X_3 + 3.41X_1X_2 + 1.14X_2X_3 + 2.63X_1X_3 - 6.45X_1X_2X_3$	(17)
Mathematical model in real coordinates	
$Y(\%) = 66.99 - 14.40Q - 421.18C - 15.51S + 6{,}542.5QC + 270.38CS + 329.56QS - 8{,}062.5QCS$	(18)

ΔG values which indicates that the sorption process of UO_2^{2+} ions is spontaneous.

The highest extraction yield was investigated by means of $3^{(3-1)}$ factorial design studies. It provided by experiment: w(mA-IRA-93) = 0.01 g, $[UO_2^{2+}] = 10^{-5}$ mol L^{-1} and $[CH_3COONa]$ = 0.2 mol L^{-1}; and w(mA-IRA-93) = 0.03 g, $[UO_2^{2+}] = 10^{-5}$ mol L^{-1} and $[CH_3COONa]$ = 1.0 mol L^{-1}. The polynomial model developed herein for the uranium(VI) SPE yield may provide a valuable basis for industrial scale applications.

In view of the results obtained in this study, these resins can be a promising as new sorption materials for immobilization and pre-concentration of rare earth elements, radioactive metal and heavy metal ions from large solutions volume. The proposed adsorbents is cost-effective and environmentally friendly and a potential candidates for treatment of water containing UO_2^{2+}. The functionalized adsorbent (mA-IRA-93) has research value and application potential in real waste water treatment.

Acknowledgements

We gratefully also acknowledge the DGRSDT - Algeria for the financial support.

Conflict of interest

The authors declare that they have no conflict of interest.

Symbol

Y (%) — Extraction yield
C_i — Initial uranium concentration
C_e — Equilibrium uranium concentration
C_t — Uranium concentration at time t
q_t — Amount of metal uptakes
V — Volume of the solution
w — Mass of resin
K_D — Distribution coefficient
$[M]_{resin}$ — UO_2^{2+} ions concentrations in resin phase
$[M]_{aq}$ — UO_2^{2+} ions concentrations in aqueous solution

References

[1] S. Nait-Tahar, M.A. Didi, Uranium micelle-mediated extraction in acetate medium: factorial design optimization, J. Radioanal. Nucl. Chem., 293 (2012) 789–795.
[2] K. Zhu, C. Chen, H. Wang, Y. Xie, M. Wakeel, A. Wahid, X. Zhang, Gamma-ferric oxide nanoparticles decoration onto porous layered double oxide belts for efficient removal of uranyl, J. Colloid Interface Sci., 535 (2019) 265–275.
[3] A. Asic, A. Kurtovic-Kozarica, L. Besic, L. Mehinovic, A. Hasic, M. Kozaric, M. Hukic, D. Marjanovic, Chemical toxicity and radioactivity of depleted uranium: the evidence from in vivo and in vitro studies, Environ. Res., 156 (2017) 665–673.
[4] L.C. Alves, U. Borgmann, D.G. Dixon, Kinetics of uranium uptake in soft water and the effect of body size, bioaccumulation and toxicity to *Hyalella azteca*, Environ. Pollut., 157 (2009) 2239–2247.
[5] T. Bacquart, S. Frisbie, E. Mitchell, L. Grigg, C. Cole, C. Small, B. Sarkar, Multiple in organic toxic substances contaminating the ground water of Myingyan Township, Myanmar: arsenic, manganese, fluoride, iron, and uranium, Sci. Total Environ., 517 (2015) 232–245.
[6] N. Gao, Z. Huang, H. Liu, J. Hou, X. Liu, Advances on the toxicity of uranium to different organisms, Chemosphere, 237 (2019) 124548, doi: 10.1016/j.chemosphere.2019.124548.
[7] P. Kurttio, A. Harmoinen, H. Saha, L. Salonen, Z. Karpas, H. Komulainen, Kidney toxicity of ingested uranium from drinking water, Am. J. Kidney Dis., 47 (2006) 972–982.

[8] J.K. Fawell, E. Ohanian, M. Giddings, P. Toft, Y. Magara, P. Jackson, World Health Organization, Uranium in Drinking Water: Chemical Fact Sheets of WHO Guidelines for Drinking-Water Quality, 3rd ed., 2004, WHO/SDE/WSH/03.04/118.
[9] Y. Sun, R. Zhang, C. Ding, X. Wang, W. Cheng, C. Chen, X. Wang, Adsorption of U(VI) on sericite in the presence of *Bacillus subtilis*: a combined batch, EXAFS and modeling techniques, Geochim. Cosmochim. Acta, 180 (2016) 51–65.
[10] H. Mei, X. Tan, S. Yu, X. Ren, C. Chen, X. Wang, Effect of silicate on U(VI) sorption to c-Al_2O_3: batch and EXAFS studies, Chem. Eng. J., 269 (2015) 371–378.
[11] H. Wang, R. Yang, X. Hua, W. Zhao, W. Zhang, Enzymatic production of lactulose and 1-lactulose: current state and perspectives, Appl. Microbiol. Biotechnol., 97 (2013) 6167–6180.
[12] Z. Li, Z. Huang, W. Guo, L. Wang, L. Zheng, Z. Chai, W. Shi, Enhanced photocatalytic removal of Uranium(VI) from aqueous solution by magnetic TiO_2/Fe_3O_4 and its graphene composite, Environ. Sci. Technol., 51 (2017) 5666–5674.
[13] P. Gu, S. Zhang, X. Li, X. Wang, T. Wen, R. Jehan, A. Alsaidi, T. Hayat, X. Wang, Recent advances in layered double hydroxide-based nanomaterials for the removal of radionuclides from aqueous solution, Environ. Pollut., 240 (2018) 493–505.
[14] H. Liu, Y. Zhu, B. Xu, P. Li, Y. Sun, T. Chen, Mechanical investigation of U(VI) on pyrrhotite by batch, EXAFS and modeling techniques, J. Hazard. Mater., 322 (2017) 488–498.
[15] A. Rekkab, M.A. Didi, Selective liquid-solid extraction of Cr(III) from Cr(III) and Fe(III) mixture by Chelex 100 resin, Sci. Stud. Res. Chem. Eng., 20 (2019) 63–74.
[16] A. Rekkab, M.A. Didi, Liquid–solid extraction of Hg(II) from aqueous solution by chelating resin chelex-100, Eur. Chem. Bull., 3 (2014) 860–868.
[17] H. Bendiaf, O. Abderrahim, D. Villemin, M.A. Didi, Studies on the feasibility of using a novel phosphonate resin for the separation of U(VI), La(III) and Pr(III) from aqueous solutions, J. Radioanal. Nucl. Chem., 312 (2017) 587–597.
[18] Md. R. Awual, T. Yaita, S. Suzuki, H. Shiwaku, Ultimate selenium(IV) monitoring and removal from water using a new class of organic ligand based composite adsorbent, J. Hazard. Mater., 291 (2015) 111–119.
[19] K. Oukebdane, O. Belyouci, M.A. Didi, Liquid–solid adsorption of Cd(II) by maghemite, Curr. Nanomater., 3 (2018) 95–102.
[20] (a) J. Sung-Ho, K. Young-UK, K. Jin-Gu, J. Rajesh Kumar, Y. Ho-Sung, P.K. Parhi, S. Shun Myung, Recovery of rhenium and molybdenum from molybdenite roasting dust leaching solution by ion exchange resins, Mater. Trans., 53 (2012) 2034–2037.
(b) S. Sinha, S.S. Behera, S. Das, A. Basu, R.K. Mohapatra, B.M. Murmu, N.K. Dhal, S.K. Tripathy, Removal of Congo red dye from aqueous solution using Amberlite IRA-400 in batch and fixed bed reactors, Chem. Eng. Commun., 205 (2018) 432–444.
[21] A. Kadous, M.A. Didi, A new sorbent for uranium extraction: ethylenediamino tris(methylenephosphonic) acid grafted on polystyrene resin, J. Radioanal. Nucl. Chem., 284 (2010) 431–438.
[22] S. Kumar, M. Krishnakumar, A.A. Patwardhan, Liquid–solid extraction of uranium(VI) with TOPO-molten naphthalene and determination by laser fluorimetry in geological samples, Explor. Res. Atomic Miner., 17 (2007) 15–21.
[23] C. Manish, C. Niharendu, Adsorption of uranyl ions from its aqueous solution by functionalized carbon nanotubes: a molecular dynamics simulation study, J. Mol. Liq., 294 (2019) 111569, doi: 10.1016/j.molliq.2019.111569.
[24] M. Ghaedi, K. Niknam, S. Zamani, H. Abasi Larki, M. Roosta, M. Soylak, Silica chemically bonded N-propyl kriptofix 21 and 22 with immobilized palladium nanoparticles for solid phase extraction and preconcentration of some metal ions, Mater. Sci. Eng. C, 33 (2013) 3180–3189.
[25] J. Gladis, T. Rao, Solid phase extractive pre-concentration of uranium on to 5,7-dichloroquinoline-8-ol modified naphthalene, Anal. Lett., 35 (2002) 501–515.
[26] M.S. Hosseini, A. Hosseini-Bandegharaei, Comparison of sorption behavior of Th(IV) and U(VI) on modified impregnated resin containing quinizarin with that conventional prepared impregnated resin, J. Hazard. Mater., 190 (2011) 755–765.
[27] A. Hosseini-Bandegharaei, M. Hosseini, Y. Jalalabadi, M. Nedai, M. Sarwghadi, A. Taherian, E. Hosseini, A novel extractant-impregnated resin containing carminic acid for selective separation and pre-concentration of uranium(VI) and thorium(IV), Int. J. Environ. Anal. Chem., 93 (2011) 108–124.
[28] M. Korn, A. Santos, H. Jaeger, N. Silva, A. Costa, Copper, zinc and manganese determination in saline samples employing FAAS after separation and preconcentration on Amberlite XAD-7 and Dowex 1X-8 loaded with Alizarin Red S, J. Braz. Chem. Soc., 15 (2004) 212–218.
[29] M. Hosseini, A. Bazrafshan, A. Hosseini-Bandegharaei, A novel solvent-impregnated resin containing 3-hydroxy-2-naphthoic acid for stepwise extraction of Th(IV) and U(VI) over other coexistence ions, Sep. Sci. Technol., 51 (2016) 1328–1335.
[30] H. Fouad, S.A. Elenein, A. Orabi, S. Abdulmoteleb, A new extractant impregnated resin for separation of traces of uranium and thorium followed by their spectrophotometric determination in some geological samples, SN Appl. Sci., 309 (2019), doi: 10.1007/s42452-019-0325-7.
[31] M. Bissen, T. Gremm, U. Köklü, F.H. Frimmel, Use of the anion-exchange resin Amberlite IRA-93 for the separation of arsenite and arsenate in aqueous samples, Acta Hydrochim. Hydrobiol., 28 (2000) 41–46.
[32] P. Yong, H. Eccles, L.E. Macaskie, Determination of uranium, thorium and lanthanum in mixed solutions using simultaneous spectrophotometry, Anal. Chim. Acta, 329 (1996) 173–179.
[33] S.I. El-Dessouky, E.A. El-Sofany, J.A. Daoud, Studies on the sorption of praseodymium(III), holmium(III) and cobalt(II) from nitrate medium using TVEX–PHOR resin, J. Hazard. Mater., 143 (2007) 17–23.
[34] M.H. Khan, P. Warwick, N. Evans, Spectrophotometric determination of uranium with arsenazo-III in perchloric acid, Chemosphere, 63 (2006) 1165–1169.
[35] D. Villemin, C. Monteil, N. Bar, M.A. Didi, Phosphonated polyethyleneimines (PEIP) as multi-use polymers, Phosphorus Sulfur, 190 (2015) 879–890.
[36] M.C. Zenobi, C.V. Luengo, M.J. Avena, E.H. Rueda, An ATR-FTIR study of different phosphonic acids in aqueous solution, Spectrochim. Acta, Part A, 70 (2007) 270–276.
[37] W. Kuang, Y.N. Liu, J. Huang, Phenol-modified hyper-cross-linked resins with almost all micro/mesopores and their adsorption to aniline, J. Colloid Interface Sci., 487 (2017) 31–37.
[38] I. Puigdomenech, MEDUSA (Make Equilibrium Diagrams Using Sophisticated Algorithms) Program, Royal Institute of Technology, Stockholm. Available at: http://www.kemi.kth.se/medusa/
[39] F. Chi, X. Wang, J. Xiong, S. Hu, Polyvinyl alcohol fibers with functional phosphonic acid group: synthesis and adsorption of uranyl(VI) ions in aqueous solutions, J. Radioanal. Nucl. Chem., 296 (2013) 1331–1340.
[40] A. Miraoui, M.A. Didi, Thorium(IV) sorption onto sodium bentonite and magnetic bentonite, Eur. Chem. Bull., 4 (2015) 512–521.
[41] N. Ferrah, O. Abderrahim, M.A. Didi, D. Villemin, Sorption efficiency of a new sorbent towards uranyl: phosphonic acid grafted Merrifield resin, J. Radioanal. Nucl. Chem., 289 (2011) 721–730.
[42] V.C. Srivastava, I.D. Mall, I.M. Mishra, Adsorption of toxic metal ions onto activated carbon Study of sorption behaviour through characterization and kinetics, Chem. Eng. Proc., 47 (2007) 1269–1280.
[43] (a) A.R. Kul, H. Koyuncu, Adsorption of Pb(II) ions from aqueous solution by native and activated bentonite: kinetic, equilibrium and thermodynamic study, J. Hazard. Mater., 179 (2010) 332–339.
(b) Md. Munjur Hasan, Md. Nazmul Hasan, Md. Rabiul Awual, Md. Mominul Islam, M.A. Shenashen, J. Iqbal, Biodegradable natural carbohydrate polymeric sustainable adsorbents for efficient toxic dye removal from wastewater, J. Mol. Liq., 319 (2020) 114356, doi: 10.1016/j.molliq.2020.114356.

[44] M. Ahmadi, R. Yavari, A.Y. Faal, H. Aghayan, Preparation and characterization of titanium tungstophosphate immobilized on mesoporous silica SBA-15 as a new inorganic composite ion exchanger for the removal of lanthanum from aqueous solution, J. Radioanal. Nucl. Chem., 310 (2016) 177–190.
[45] L. Huang, L. Zhang, D. Hua, Synthesis of polyamidoxime-functionalized nanoparticles for uranium(VI) removal from neutral aqueous solutions, J. Radioanal. Nucl. Chem., 305 (2015) 445–453.
[46] A. Kadous, M.A. Didi, D. Villemin, Removal of uranium(VI) from acetate medium using Lewatit TP 260 resin, J. Radioanal. Nucl. Chem., 288 (2011) 553–561.
[47] S. Katragadda, H.D. Gesser, A. Chow, Extraction of uranium from aqueous solution by phosphonic acid-imbedded polyurethane foam, Talanta, 44 (1997) 1865–1871.
[48] P. Joaquim, Marques de Sá, Applied Statistics Using SPSS, STATISTICA, MATLAB and R, ISBN 978-3-540-71971-7, Springer, Berlin, Heidelberg, New York, 2007.